bioRxiv preprint doi: https://doi.org/10.1101/2020.05.08.084616; this version posted May 10, 2020. The copyright holder for this preprint (which was not certified by peer review) is the author/funder, who has granted bioRxiv a license to display the preprint in perpetuity. It is made available under a CC-BY-NC-ND 4.0 International license.

History of childbirths relates to region-specific brain aging patterns in middle and older-aged women

Ann-Marie G. de Lange[1,2,3*], **Claudia Barth**[3], **Tobias Kaufmann**[3], **Melis Anatürk**[1,4], **Sana Suri**[1,4], **Klaus P. Ebmeier**[1], **Lars T. Westlye**[2,3,5]

***For correspondence:** ann-marie.delange@psych.ox.ac.uk

Present address: Department of Psychiatry, University of Oxford, Oxford, UK

[1]Department of Psychiatry, University of Oxford, Oxford, UK; [2]Department of Psychology, University of Oslo, Oslo, Norway; [3]NORMENT, Institute of Clinical Medicine, University of Oslo, & Division of Mental Health and Addiction, Oslo University Hospital, Oslo, Norway; [4]Wellcome Centre for Integrative Neuroimaging, University of Oxford, Oxford, UK; [5]KG Jebsen Centre for Neurodevelopmental Disorders, University of Oslo, Oslo, Norway

Abstract Pregnancy involves maternal brain adaptations, but little is known about how parity influences women's brain aging trajectories later in life. In this study, we replicated previous findings showing less apparent brain aging in women with a history of childbirths, and identified regional brain aging patterns linked to parity in 19,787 middle and older-aged women. Using novel applications of brain-age prediction methods, we found that a higher number of previous childbirths was linked to less apparent brain aging in striatal and limbic regions. The strongest effect was found in the accumbens - a key region in the mesolimbic reward system, which plays an important role in maternal behavior. While only prospective longitudinal studies would be conclusive, our findings indicate that subcortical brain modulations during pregnancy and postpartum may be traceable decades after childbirth.

Introduction

Pregnancy involves a number of maternal brain adaptations (***Barha and Galea, 2017***; ***Fox et al., 2018***; ***Hillerer et al., 2014***; ***Eid et al., 2019***; ***Boddy et al., 2015***). In rodents, changes in volume, cell proliferation, and dendritic morphology (***Hillerer et al., 2014***; ***Kinsley et al., 2006***), as well as altered neurogenesis in the hippocampus (***Eid et al., 2019***; ***Rolls et al., 2008***) are found across pregnancy and postpartum. In humans, reduction in total brain volume has been observed during pregnancy, reversing within six months of parturition (***Oatridge et al., 2002***). Reductions in striatal volumes, particularly putamen, have been reported shortly after delivery (***Lisofsky et al., 2016***), and pregnancy-related reductions in gray matter volume have been found in regions subserving social cognition; the bilateral lateral prefrontal cortex, the anterior and posterior midline, and the bilateral temporal cortex (***Hoekzema et al., 2017***). Conversely, a recent study showed no evidence of decrease in gray matter volume following childbirth, but instead detected a pronounced gray matter *increase* in both cortical and subcortical regions (***Luders et al., 2020***). Prefrontal cortical thickness and subcortical volumes in limbic areas have been positively associated with postpartum months (***Kim et al., 2018***), indicating that changes in brain structure may depend on region and time since delivery (***Luders et al., 2020***; ***Duarte-Guterman et al., 2019***; ***Hoekzema et al., 2017***; ***Kim et al., 2018***, ***2010***). For instance, from 2–4 weeks to 3–4 months postpartum, gray matter volume

bioRxiv preprint doi: https://doi.org/10.1101/2020.05.08.084616; this version posted May 10, 2020. The copyright holder for this preprint (which was not certified by peer review) is the author/funder, who has granted bioRxiv a license to display the preprint in perpetuity. It is made available under a CC-BY-NC-ND 4.0 International license.

increases have been found in areas involved in maternal behaviours and motivation, such as the amygdala, substantia nigra, hypothalamus, and prefrontal cortex (***Kim et al., 2010***).

While gray matter reductions have been reported up to 2 years post-pregnancy, most studies are limited to the postpartum period, and little is known about how previous pregnancies influence women's brain aging later in life. Evidence from animal studies shows that middle-aged multiparous rats have stronger cellular response to estrogens in the hippocampus compared to virgin female rats (***Barha and Galea, 2011***), suggesting that neuroplastic potential across the adult lifespan may be influenced by previous pregnancies. Moreover, hippocampal neurogenesis has been shown to increase during middle age in primiparous rats and decrease in nulliparous rats over the same period (***Eid et al., 2019***). While longitudinal studies on parity and brain aging in humans are lacking, cumulative number of months pregnant has been associated with decreased risk for Alzheimer's disease (***Fox et al., 2018***), and we recently documented less evident brain aging in parous relative to nulliparous women in >12,000 UK Biobank participants using an magnetic resonance imaging (MRI)-derived biomarker of global brain aging (***de Lange et al., 2019***).

In the current study, we first aimed to replicate our previously reported findings described in ***de Lange et al.*** (***2019***), where less apparent brain aging was found in women with a history of childbirths. Brain-age prediction methods were used to derive estimates of global brain aging, which was analysed in relation to number of previous (live) childbirths in 8880 newly added UK Biobank participants. Brain-age prediction is commonly used to estimate an individual's age based on their brain characteristics (***Cole and Franke, 2017***), and individual variation in "brain age" estimates has been associated with a range of clinical and biological factors (***Cole and Franke, 2017***; ***Kaufmann et al., 2019***; ***Franke and Gaser, 2019***; ***Cole et al., 2018***, ***2019***; ***Cole, 2019***; ***Smith et al., 2019***; ***Cole et al., 2017***; ***de Lange et al., 2020a***,b). As compared to MRI-derived measures such as cortical volume or thickness, brain-age prediction adds a dimension by capturing deviations from normative trajectories identified by machine learning. While traditional brain age approaches summarize measures across regions to produce a single, global aging estimate - often with high prediction accuracy, models of distinct and regional aging patterns can provide more refined biomarkers that may capture additional biological detail (***Kaufmann et al., 2019***; ***Smith et al., 2020***; ***Eavani et al., 2018***). In this study, we utilized novel applications of brain-age prediction methods based on cortical and subcortical volumes to identify regions of particular importance for maternal brain aging, using a total sample of 19,787 UK Biobank women.

Results

Associations between previous childbirths and global brain aging:

To replicate our findings described in ***de Lange et al.*** (***2019***), we trained a brain-age prediction model on the part of the current sample that overlapped with the previous study (N = 10,907), and applied it to the newly added participants (N = 8880) using the procedure described in *Methods and Materials*. When applied to the test set, the modeled age prediction showed an accuracy of R^2 = 0.34, root mean square error (RMSE) = 6.00, and Pearson's r (predicted versus chronological age) = 0.58; 95% confidence interval (CI) = [0.57, 0.59], $p < 0.001$. Corresponding to our previous results, an association was found between a higher number of previous childbirths and less apparent brain aging in the group of newly added participants: $\beta = -0.13$ standard error (SE) = 0.03, $t = -4.07, p = 4.79\times10^{-5}$. To adjust for age-bias in the brain age prediction as well as age-dependencies in number of childbirths (***Le et al., 2018***), chronological age was included as a covariate in the linear regression.

To test for non-linear relationships, polynomial fits were run for number of childbirths and brain age gap; one including intercept and a linear term (β) only, and one including intercept, linear, and quadratic terms (γ). For these analyses, the brain age gap estimations were first corrected for chronological age using linear regression (***Le et al., 2018***), and the residuals were used in the fits. A comparison of the two models showed that the inclusion of the quadratic term did not provide a better fit ($F = 0.06, p = 0.804$). The results from the fit including the linear term only showed

bioRxiv preprint doi: https://doi.org/10.1101/2020.05.08.084616; this version posted May 10, 2020. The copyright holder for this preprint (which was not certified by peer review) is the author/funder, who has granted bioRxiv a license to display the preprint in perpetuity. It is made available under a CC-BY-ND 4.0 International license.

a significant linear effect ($\beta = -0.12 \pm 0.03; F = 16.10, p = 6.05 \times 10^{-5}$), while the results from the fit including both terms showed that only the linear term was significant ($\beta = -0.14 \pm 0.072; \gamma = 0.004 \pm 0.02; F = 8.08, p = 3.11 \times 10^{-4}$). The two fits are shown in Figure 1. As a cross check, the fits were rerun with orthogonal polynomials, showing corresponding results ($\beta = -13.44 \pm 3.35$, $\gamma = 0.83 \pm 3.35; F = 8.08, p = 3.11 \times 10^{-4}$).

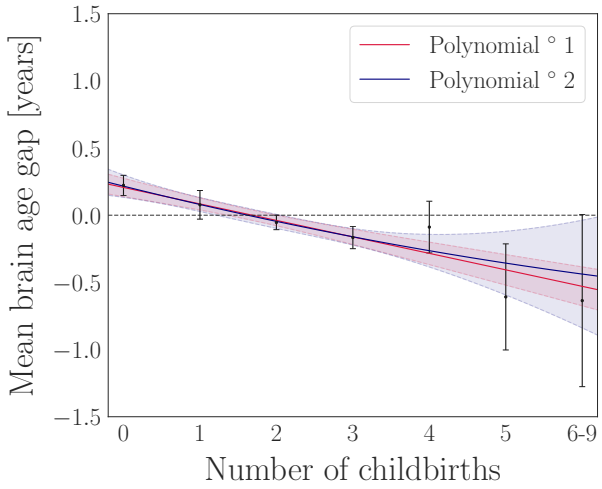

Figure 1. Results from first and second degree polynomial fits for number of childbirths and global brain aging in the newly added participants (N = 8880). The black points indicate the mean brain age gap ± standard error within groups of women based on number of childbirths (x-axis). The red and blue lines represent the results of the fits, and the shaded areas indicate the ± 95% confidence intervals for each fit. The horizontal dashed line indicates 0 on the y-axis. Number of participants in each group: 0 births = 2065, 1 birth = 1014, 2 births = 3912, 3 births = 1493, 4 births = 311, 5 births = 67, 6 births = 13, 7 births = 3, 8 births = 1, and 9 births = 1. The group of women with 6-9 children were merged to obtain sufficient statistics for least square fits using the standard error on the means as weights.

Regional brain aging patters:

To identify groups of imaging features based on their covariance, we performed hierarchical clustering on the Spearman rank-order correlations using an average of right and left hemisphere measures for each feature. Five clusters were identified, as shown in Figure 2. All features were grouped according to their associated cluster ID, and separate models were run to estimate brain age for each cluster using the brain-age prediction procedure described in *Methods and Materials*. The features contained in each cluster are listed in Table 1. The cluster-specific model performances are shown in Table 2.

To test whether the relative prediction accuracy of the models depended on number of features, the models were rerun using the four strongest contributing features from each model as input variables. The feature contributions were calculated using permutation feature importance, defining the decrease in model performance when a single feature value is randomly shuffled (***Breiman, 2001***). The results are shown in Table 3.

bioRxiv preprint doi: https://doi.org/10.1101/2020.05.08.084616; this version posted May 10, 2020. The copyright holder for this preprint (which was not certified by peer review) is the author/funder, who has granted bioRxiv a license to display the preprint in perpetuity. It is made available under a CC-BY-ND 4.0 International license.

Figure 2. Dendrogram based on hierarchical clustering on the Spearman rank-order correlations of all features. The colours represent clusters (C) of features that are grouped together based on common covariance. A list of imaging features contained in each of the clusters are provided in Table 1. The y-axis shows the degree of co-linearity between the features, with higher y-values indicating less co-linearity between clusters.

Table 1. List of imaging features contained in each of the clusters identified based on hierarchical clustering (Figure 2). All feature names represent regional volume.

Cluster 1			
Cuneus	Isthmuscingulate	Lateraloccipital	Lingual
Pericalcarine	Precuneus	Superiorparietal	
Cluster 2			
Caudalanteriorcingulate	Lateralorbitofrontal	Medialorbitofrontal	Paracentral
Parsopercularis	Parsorbitalis	Parstriangularis	Postcentral
Posteriorcingulate	Precentral	Rostralmiddlefrontal	Superiorfrontal
Superiortemporal	Supramarginal	Transversetemporal	Insula
Cluster 3			
Banks of superior temporal sulcus	Fusiform	Inferiorparietal	Inferiortemporal
Middletemporal	Parahippocampal	Thalamus	Putamen
Hippocampus	Amygdala	Accumbens	
Cluster 4			
Caudalanteriorcingulate	Entorhinal	Rostralanteriorcingulate	Frontalpole
Temporalpole			
Cluster 5			
Brain-Stem	Cerebellum	Caudate	Pallidum

bioRxiv preprint doi: https://doi.org/10.1101/2020.05.08.084616; this version posted May 10, 2020. The copyright holder for this preprint (which was not certified by peer review) is the author/funder, who has granted bioRxiv a license to display the preprint in perpetuity. It is made available under a CC-BY-NC-ND 4.0 International license.

Table 2. The accuracy of the age prediction measured by Pearson's r (predicted versus chronological age), R^2, root mean square error (RMSE), and mean absolute error (MAE) for each of the cluster-specific models. 95 % confidence intervals are indicated in square brackets. RMSE and MAE are reported in years. N_{feat} = number of features contained in the cluster. *P*-values were < 0.001 for all models.

Model	N_{feat}	r	R^2	RMSE	MAE
Cluster 1	7	0.32 [0.31, 0.33]	0.10 [0.10, 0.11]	7.00	5.79
Cluster 2	16	0.38 [0.36, 0.39]	0.14 [0.13, 0.15]	6.86	5.64
Cluster 3	11	0.48 [0.47, 0.49]	0.23 [0.23, 0.24]	6.48	5.29
Cluster 4	5	0.13 [0.11, 0.14]	0.02 [0.01, 0.02]	7.36	6.13
Cluster 5	4	0.21 [0.19, 0.22]	0.04 [0.04, 0.05]	7.25	6.04

Table 3. The accuracy of the age prediction when including the four strongest contributing features for each model. 95 % confidence intervals are indicated in square brackets. RMSE and MAE are reported in years. N_{feat} = number of features included. *P*-values were < 0.001 for all models.

Model	N_{feat}	r	R^2	RMSE	MAE
Cluster 1	4	0.32 [0.31, 0.33]	0.10 [0.10, 0.11]	7.01	5.80
Cluster 2	4	0.34 [0.33, 0.35]	0.11 [0.11, 0.12]	6.96	5.75
Cluster 3	4	0.46 [0.45, 0.47]	0.21 [0.21, 0.22]	6.55	5.36
Cluster 4	4	0.12 [0.11, 0.13]	0.02 [0.01, 0.02]	7.36	6.14
Cluster 5	4	0.21 [0.19, 0.22]	0.04 [0.04, 0.05]	7.25	6.04

Associations between previous childbirths and regional brain aging:

The cluster-specific associations with number of previous childbirths are shown in Table 4.

Table 4. Relationships between number of previous childbirths and estimated brain aging for each cluster. Cluster-specific *brain age gap* was entered as the dependent variable and *number of (live) childbirths* was entered as independent variable for each analysis. Chronological age was included for covariate purposes. *P*-values are provided before and after FDR correction. Significant relationships (< 0.05) are marked with an asterisk in the p_{corr} column. SE = standard error.

Number of childbirths vs cluster-specific brain age estimates					
Cluster	β	SE	t	p	p_{corr}
1	-0.054	0.016	-3.282	0.001	0.002*
2	-0.010	0.018	-0.552	0.581	0.726
3	-0.133	0.021	-6.385	1.754×10^{-10}	8.768×10^{-10}*
4	-0.003	0.010	-0.278	0.781	0.781
5	-0.056	0.012	-4.620	3.868×10^{-16}	9.670×10^{-6}*

As shown in Table 4, brain aging estimates based on three clusters were each significantly associated with number of previous childbirths. To test whether the associations were statistically different from each other, pairwise Z tests for correlated samples (Eq. 1, *Methods and Materials*) were run on the cluster-specific associations with number of childbirths. The results showed that cluster 3 was more strongly related to number of previous childbirths relative to the other clusters, as shown in Figure 3.

bioRxiv preprint doi: https://doi.org/10.1101/2020.05.08.084616; this version posted May 10, 2020. The copyright holder for this preprint (which was not certified by peer review) is the author/funder, who has granted bioRxiv a license to display the preprint in perpetuity. It is made available under a CC-BY-ND 4.0 International license.

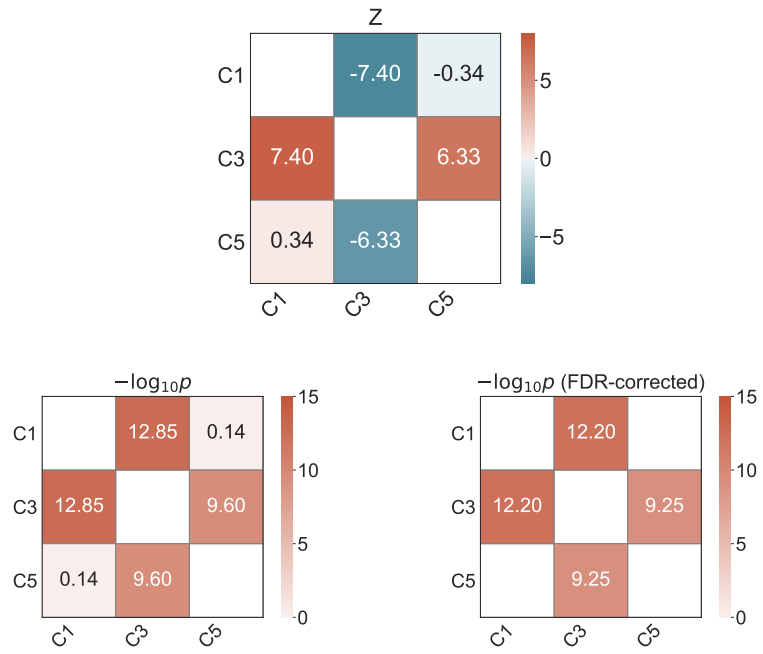

Figure 3. Top plot: Matrix showing pairwise differences between the cluster-specific associations with number of childbirths, based on Z tests for correlated samples (Eq.1). Bottom left plot: Uncorrected -Log10 p-values of the differences between the cluster-specific associations. Bottom right plot: -Log10 *p*-values corrected for multiple comparisons using FDR, with only significant values (< 0.05) displayed. C = cluster.

To investigate further specificity, the clustering procedure was repeated on the features in cluster 3 - the cluster showing the strongest association with number of childbirths. Two subclusters were identified based on the covariance of the features, as shown in Figure 4. Subcluster 1 included 5 features; subcluster 2 included 6 features. The features were matched with the cluster they belonged to, and separate models were run to generate brain-age predictions for each subcluster. The subcluster-specific model performances are shown in Table 5, and their associations with number of previous childbirths are shown in Table 6.

Table 5. The accuracy of the age prediction measured by Pearson's r (predicted versus chronological age), R^2, root mean square error (RMSE), and mean absolute error (MAE) for each of the subcluster-specific models. 95 % confidence intervals are indicated in square brackets. RMSE and MAE are reported in years. N_{feat} = number of features contained in the cluster. P-values were < 0.001 for both models.

Model	N_{feat}	r	R^2	RMSE	MAE
Subcluster 1	5	0.33 [0.31, 0.34]	0.11 [0.10, 0.12]	6.99	5.79
Subcluster 2	6	0.47 [0.45, 0.48]	0.22 [0.20, 0.23]	6.54	5.35

bioRxiv preprint doi: https://doi.org/10.1101/2020.05.08.084616; this version posted May 10, 2020. The copyright holder for this preprint (which was not certified by peer review) is the author/funder, who has granted bioRxiv a license to display the preprint in perpetuity. It is made available under a CC-BY-ND 4.0 International license.

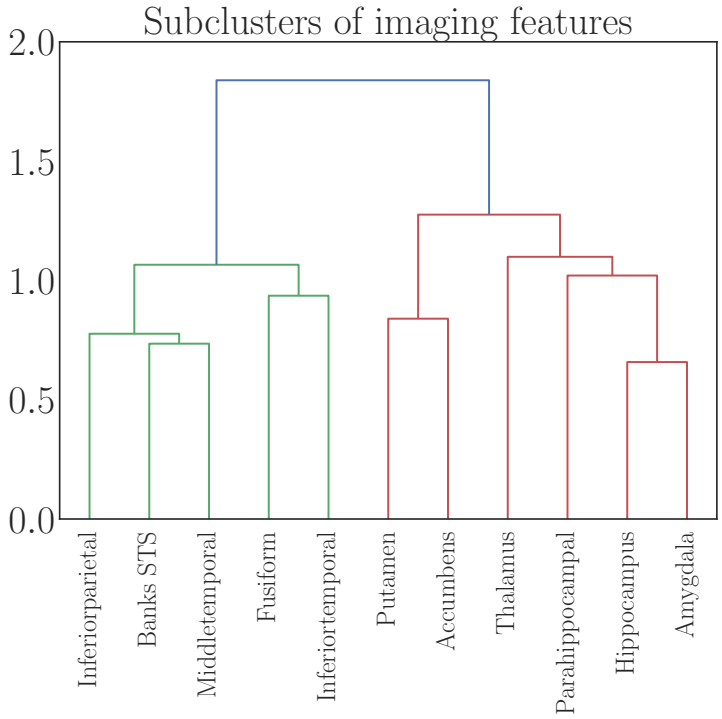

Figure 4. Dendrogram based on hierarchical clustering on the Spearman rank-order correlations of the features contained in Cluster 3, which showed the strongest association with number of childbirths (see Figure 3). The colours represent clusters of features that are grouped together based on common covariance; subcluster 1 in green and subcluster 2 in red. The y-axis shows the degree of co-linearity between the features, with higher y-values indicating less co-linearity between clusters. STS = superior temporal sulcus.

Table 6. Relationships between number of previous childbirths and estimated brain aging for each subcluster. Subcluster-specific *brain age gap* was entered as the dependent variable and *number of childbirths* was entered as independent variable for each analysis. Chronological age was included for covariate purposes. *P*-values are provided before and after FDR correction.

Number of childbirths vs subcluster-specific brain age estimates					
Subcluster	β	SE	t	p	p_{corr}
1	-0.071	0.016	-4.321	1.563×10^{-5}	1.563×10^{-5}
2	-0.124	0.020	-6.169	7.024×10^{-10}	1.405×10^{-9}

Table 7. Difference in quadrature between the subcluster-specific associations with number of childbirths, calculated using Eq. 1 (*Methods and Materials*).

Comparison	Z	p	p_{corr}
Subcluster 1 vs subcluster 2	-5.32	1.01×10^{-7}	2.03×10^{-7}

bioRxiv preprint doi: https://doi.org/10.1101/2020.05.08.084616; this version posted May 10, 2020. The copyright holder for this preprint (which was not certified by peer review) is the author/funder, who has granted bioRxiv a license to display the preprint in perpetuity. It is made available under a CC-BY-ND 4.0 International license.

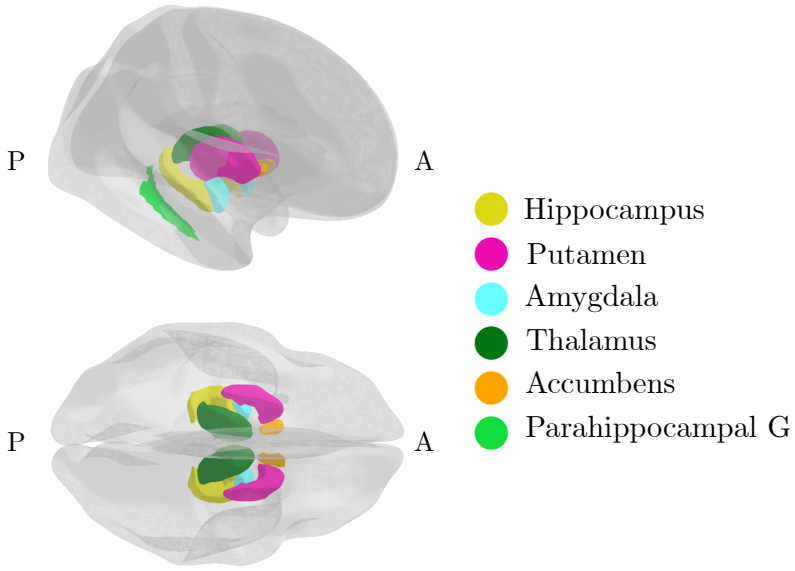

Figure 5. Regions in subcluster 2 - the cluster that showed the strongest association with number of previous childbirths. A = anterior, G = gyrus, P = posterior. Figure created using the *ggseg* plotting tool for brain atlases in R (***Mowinckel and Vidal-Piñeiro, 2019***).

To control for potential confounding factors, the analyses of number of previous childbirths versus subcluster 2 brain age estimates were rerun including assessment location, education, body mass index (BMI), diabetic status, hypertension, smoking and alcohol intake, menopausal status ('yes', 'no', 'not sure, had hysterectomy', and 'not sure, other reason'), and oral contraceptive (OC) and hormonal replacement therapy (HRT) status (previous or current user vs never used) as covariates. 16,512 women had data on all variables and were included in the analyses. The results showed an association of $\beta = -0.12$, SE $= 0.02, t = -5.36, p = 8.27 \times 10^{-8}$ between number of childbirths and subcluster 2, indicating that the covariates could not fully explain the association. Number of previous childbirths and age at first birth correlated $r = -0.294, p = 6.90 \times 10^{-296}$ (corrected for age). To test for an association with brain aging, an analysis was run with subcluster 2 brain age as the dependent variable and *age at first birth* as independent variable, including all the covariates (age, assessment location, education, BMI, diabetic status, hypertension, smoking and alcohol intake, menopausal status, OC and HRT use). No association was found ($\beta = 0.010$, SE $= 0.01, t = 1.64, p = 0.102$, N $= 12,937$).

Single-region associations:

To investigate the unique contributions of each region in subcluster 2 to the association with previous childbirths, separate brain-age prediction models were run with each feature as input, yielding 11 region-specific brain age estimates. Table 8 shows the correlation between predicted and chronological age for each region-specific model, and their associations with number of childbirths. As the regions within the cluster were correlated (see Figure 4), we tested for unique contributions by first running a multiple regression analysis with all region-specific brain age estimates as independent variables and *number of childbirths* as the dependent variable, before eliminating the regions one at a time to compare the log-likelihood of the full and reduced models. The significance of model differences was calculated using Wilk's theorem (***Wilks, 1938***) as $\sqrt{2(\Delta LL)}$, where $\Delta LL = LL_1 - LL_2$; the difference in log-likelihood between the reduced model (LL_1) and the full model (LL_2). The results showed that only the accumbens contributed uniquely to the association

bioRxiv preprint doi: https://doi.org/10.1101/2020.05.08.084616; this version posted May 10, 2020. The copyright holder for this preprint (which was not certified by peer review) is the author/funder, who has granted bioRxiv a license to display the preprint in perpetuity. It is made available under a CC-BY-ND 4.0 International license.

with number of previous childbirths. The association when excluding accumbens from subcluster 2 was $\beta = -0.098$, SE $= 0.020, t = -5.001, p = 5.766 \times 10^{-07}$, indicating that the association was not solely driven by this region.

Table 8. Region-specific age prediction accuracy (correlation between predicted and chronological age; r_{Age}) and association with number of childbirths (β_{CB}, standard error (SE), t, p, and p_{corr}) for each of the region-specific brain age gap estimates. Chronological age was included in the analyses for covariate purposes. 95 % confidence intervals are indicated in square brackets. *P*-values are reported before and after FDR correction.

Subcluster 2 region	r_{Age}	β_{CB}	SE	t	p	p_{corr}
Parahippocampal	0.24 [0.23, 0.25]	-0.020	0.012	-1.650	0.099	0.099
Thalamus	0.35 [0.34, 0.36]	-0.048	0.016	-2.991	0.003	0.003
Putamen	0.24 [0.22, 0.25]	-0.053	0.012	-4.401	1.08×10^{-5}	2.253×10^{-5}
Hippocampus	0.33 [0.32, 0.34]	-0.061	0.016	-3.923	8.77×10^{-5}	1.315×10^{-4}
Amygdala	0.29 [0.27, 0.30]	-0.061	0.014	-4.393	1.13×10^{-5}	2.252×10^{-5}
Accumbens	0.31 [0.30, 0.32]	-0.101	0.015	-6.812	9.90×10^{-12}	5.937×10^{-11}

Table 9. Difference in log-likelihood (ΔLL) between regression analyses against *number of children*. The difference is calculated between models where all cluster features are included and models where single features are left out one at the time. *P*-values are reported before and after FDR correction.

Left-out feature	ΔLL	Z	p	p_{corr}
Parahippocampal	0.051	0.322	0.758	0.758
Thalamus	0.753	1.227	0.376	0.563
Putamen	1.819	1.907	0.129	0.388
Hippocampus	0.352	0.839	0.561	0.673
Amygdala	0.813	1.275	0.354	0.563
Accumbens	10.568	4.597	2.05×10^{-5}	1.232×10^{-4}

As a cross check, we investigated associations between previous childbirths and regional volumes in subcluster 2. Separate analyses were run with the volume measure for each region as dependent variables and number of previous childbirths as the independent variable, including age, assessment location, education, BMI, diabetic status, hypertension, smoking and alcohol intake, menopausal status, and OC and HRT status as covariates. 16,516 women had data on all variables and were included in the analysis. The associations between number of previous childbirths and regional volume corresponded to the associations with brain age estimates, as shown in Table 10.

Table 10. Relationships between number of previous childbirths and volume for each region in subcluster 2. *P*-values are provided before and after FDR correction.

Number of childbirths vs regional volume					
Region	β	SE	t	p	p_{corr}
Parahippocampal	1.730	1.647	1.051	0.293	0.293
Thalamus	7.364	3.627	2.030	0.042	0.051
Putamen	9.369	3.215	2.914	0.004	0.005
Hippocampus	7.359	2.295	3.207	0.001	0.003
Amygdala	4.946	1.094	4.522	6.165×10^{-6}	1.849×10^{-5}
Accumbens	3.311	0.554	5.979	2.291×10^{-9}	1.374×10^{-8}

bioRxiv preprint doi: https://doi.org/10.1101/2020.05.08.084616; this version posted May 10, 2020. The copyright holder for this preprint (which was not certified by peer review) is the author/funder, who has granted bioRxiv a license to display the preprint in perpetuity. It is made available under a CC-BY-NC-ND 4.0 International license.

Discussion

The results showed that a higher number of previous childbirths was associated with less apparent brain aging in striatal and limbic regions, including the accumbens, putamen, thalamus, hippocampus, and amygdala. The most prominent effect was seen in the accumbens, which is part of the ventral striatum and a key region in the mesolimbic system involved in reward processing and reinforcement learning (***Haber and Knutson, 2010***). The mesolimbic system plays a pivotal role in the rapid emergence of adequate maternal behavior directly after birth due to its role in motivation, reward, and the hedonic value of stimuli (***Brunton and Russell, 2008***; ***Numan and Woodside, 2010***). In rodents, this circuit is activated by pup-related cues that strongly motivate and reinforce maternal care, such as odor (***Fleming et al., 1989***), ultrasonic vocalization (***Robinson et al., 2011***), and suckling (***Ferris et al., 2005***). Low levels of maternal care have been associated with reduced dopamine release within the nucleus accumbens in response to pup cues (***Champagne et al., 2004***), and in humans, motherhood has been linked to anatomical changes in the ventral striatum, with volume reductions promoting responsivity to offspring cues (***Hoekzema et al., 2020***). Together with the ventral striatum, regions including the thalamus, parietal cortex, and brainstem also serve important functions for processing pup-related somatosensory information (***Kim et al., 2010***), and some evidence suggests that structural reorganization occurs in the thalamus, parietal lobe, and somatosensory cortex as a result of physical interactions with pups during nursing (***Kinsley et al., 2008***; ***Xerri et al., 1994***). A recent study by ***Luders et al.*** (***2020***) found an increase in regional volumes including the thalamus in women postpartum, corroborating functional MRI (fMRI) studies showing maternal thalamic activation in response to their offspring (***Paul et al., 2019***; ***Rocchetti et al., 2014***). During mother–infant interaction, brain activation has also been shown to increase in the striatum (including putamen and accumbens), amygdala, substantia nigra, insula, inferior frontal gyrus, and temporal gyrus (***Rocchetti et al., 2014***). To summarize, the brain regions identified in the current study largely overlap with neural circuitry underpinning maternal behavior, indicating that brain modulations during pregnancy and postpartum may be traceable decades after childbirth.

In addition to the regions overlapping with the maternal circuit, we found a link between hippocampal brain aging and previous childbirths. This association concurs with animal studies showing enhanced hippocampal neurogenesis in middle age in parous relative to nulliparous rats (***Eid et al., 2019***), and fewer hippocampal deposits of amyloid precursor protein in multiparous relative to primiparous and virgin animals (***Love et al., 2005***). Contrary to the findings in middle-aged animals, *reduced* hippocampal neurogenesis has been reported during the postpartum period, coinciding with enhanced memory performance in primiparous compared to nulliparous rodents (***Kinsley and Lambert, 2008***). In combination with the evidence of both increased and decreased regional volume in humans postpartum (***Luders et al., 2020***; ***Hoekzema et al., 2017***; ***Kim et al., 2018***), these findings emphasize that pregnancy-related brain changes may be highly dynamic.

Pregnancy represents a period of enhanced neuroplasticity of which several underlying mechanisms could confer long-lasting effects on the brain. Fluctuations in hormones including estradiol, progesterone, prolactin, oxytocin, and cortisol are known to influence brain plasticity (***Galea et al., 2014***; ***Simerly, 2002***; ***Barha and Galea, 2010***), and levels of estradiol - a potent regulator of neuroplasticity (***Barha and Galea, 2010***) - rise up to 300-fold during pregnancy (***Schock et al., 2016***) and fall 100–1000 fold postnatally (***Nott et al., 1976***). Hormonal modulations are closely linked to pregnancy-related immune adaptations such as the proliferation of Treg cells (***Kieffer et al., 2017***), which promotes an anti-inflammatory immune environment and contribute to the observed improvement in symptoms of autoimmune disease during pregnancy (***Whitacre et al., 1999***; ***Natri et al., 2019***). In contrast, the transition to menopause marks a period of decline in ovarian hormone levels and can foster a pro-inflammatory phenotype involving increased risk for autoimmune activity and neuronal injury. Beneficial immune adaptations in pregnancy could potentially have long-lasting effects, improving the response to menopause-related inflammation, and sub-

bioRxiv preprint doi: https://doi.org/10.1101/2020.05.08.084616; this version posted May 10, 2020. The copyright holder for this preprint (which was not certified by peer review) is the author/funder, who has granted bioRxiv a license to display the preprint in perpetuity. It is made available under a CC-BY-ND 4.0 International license.

sequently leading to more favorable brain aging trajectories in multiparous women (***Mishra and Brinton, 2018***; ***Fox et al., 2018***; ***Barth and de Lange, 2020***). Another mechanism through which pregnancy may have long-lasting effects on maternal physiology is fetal microchimerism - the presence of fetal cells in the maternal body (***Boddy et al., 2015***). In mice, fetal cells have been found in several brain regions including the hippocampus, where they mature into neurons and integrate into the existing circuitry (***Zeng et al., 2010***). Further evidence for beneficial effects of childbirths on the aging brain stems from studies showing that telomeres are significantly elongated in parous relative to nulliparous women (***Barha et al., 2016***), indicating that parity may slow the pace of cellular aging. However, parity has also been linked to Alzheimer's-like brain pathology including neurofibrillary tangle and neuritic plaque (***Beeri et al., 2009***; ***Chan et al., 2012***), as well as increased risk of Alzheimer's disease (***Beeri et al., 2009***; ***Colucci et al., 2006***), with a higher risk in grand-parous women (> 5 childbirths) (***Jang et al., 2018***). Although our previous study showed some evidence of a moderate non-linear trend between number of childbirths and global brain aging (***de Lange et al., 2019***), this effect was not replicated in the current study. More research is needed to determine whether positive effects of pregnancies are less pronounced in grand-parous women, as findings could be biased by low power due to the relatively few women with five or more childbirths, as well as confounding factors such as socioeconomic status or stress levels (***Zeng et al., 2016***).

In conclusion, the current study replicates preceding findings showing less apparent brain aging in multiparous women (***de Lange et al., 2019***), and highlights brain regions that may be particularly influenced by previous childbirths. While prospective longitudinal studies are needed to fully understand any enduring effects of pregnancy, our novel use of regional brain-age prediction - which captures deviations from normative aging - demonstrates that parity relates to region-specific brain aging patterns evident decades after a woman's last childbirth.

bioRxiv preprint doi: https://doi.org/10.1101/2020.05.08.084616; this version posted May 10, 2020. The copyright holder for this preprint (which was not certified by peer review) is the author/funder, who has granted bioRxiv a license to display the preprint in perpetuity. It is made available under a CC-BY-ND 4.0 International license.

Methods and Materials

Sample characteristics:

The sample was drawn from the UK Biobank (www.ukbiobank.ac.uk), and included an initial sample of 21,928 women. 1885 participants with known brain disorders were excluded based on ICD10 diagnose (chapter V and VI, field F; *mental and behavioral disorders* and G; *diseases of the nervous system*, except G5 (http://biobank.ndph.ox.ac.uk/showcase/field.cgi?id=41270). 220 participants were excluded based on MRI outliers (see *MRI data acquisition and processing*) and 9 had missing data on number of previous childbirths, yielding a total of 19,787 participants that were included in the analyses. Sample demographics are provided in Table 11.

Table 11. Sample demographics. GCSE = General Certificate of Secondary Education, NVQ = National Vocational Qualification.

Age	
Mean ± SD	63.59 ± 7.38
Range [years]	45.13 - 82.27
Number of childbirths (live)	
Mean ± SD	1.72 ± 1.16
Range	0 - 9
N in each group:	
0 = 4297 | **1** = 2459 | **2** = 8770	
3 = 3334 | **4** = 729 | **5** = 142	
6 = 43 | **7** = 7 | **8** = 5 | **9** = 1	
Age at first birth (N = 15,446)	
Mean ± SD	27.08 ± 5.01
Range	14 - 47
Years since last birth (N = 13,023)	
Mean ± SD	33.37 ± 9.32
Range	6.77 - 60.34
Menopausal status (N = 19,781)	
Yes	6117
No	10737
Not sure, had hystorectomy	1912
Not sure, other reason	1015
Ethnic background	
% White	97.06
% Black	0.69
% Mixed	0.54
% Asian	0.75
% Chinese	0.37
% Other	0.55
% Do not know	0.03
Education	
% University/college degree	44.71
% A levels or equivalent	14.09
% O levels/GCSE or equivalent	24.91
% NVQ or equivalent	3.17
% Professional qualification	5.65
% None of the above	5.91
Assessment location (imaging)	
Newcastle	5139
Cheadle	11906
Reading	2742

bioRxiv preprint doi: https://doi.org/10.1101/2020.05.08.084616; this version posted May 10, 2020. The copyright holder for this preprint (which was not certified by peer review) is the author/funder, who has granted bioRxiv a license to display the preprint in perpetuity. It is made available under a CC-BY-NC-ND 4.0 International license.

MRI data acquisition and processing:

A detailed overview of the UK Biobank data acquisition and protocols is available in papers by ***Alfaro-Almagro et al.*** (***2018***) and ***Miller et al.*** (***2016***). Raw T1-weighted MRI data for all participants were processed using a harmonized analysis pipeline, including automated surface-based morphometry and subcortical segmentation. Volumes of cortical and subcortical brain regions were extracted based on the Desikan-Killiany atlas (***Desikan et al., 2006***) and automatic subcortical segmentation in FreeSurfer (***Fischl et al., 2002***), yielding a set of 68 cortical features (34 per hemisphere) and 17 subcortical features (8 per hemisphere + the brain stem). The MRI data were residualized with respect to scanning site, data quality and motion using Euler numbers (***Rosen et al., 2018***) extracted from FreeSurfer, intracranial volume (***Voevodskaya et al., 2014***), and ethnic background using linear models. To remove bad quality data likely due to subject motion participants with Euler numbers of standard deviation (SD) $\pm$ 4 were identified and excluded (n = 192). In addition, participants with SD $\pm$ 4 on the global MRI measures mean cortical or subcortical gray matter volume were excluded (n = 13 and n = 22, respectively), yielding a total of 19,796 participants with T1-weighted MRI data. Only participants who had data on number of previous childbirths in addition to MRI were included, and the final sample used in all subsequent analyses (unless otherwise stated) counted 19,787 participants.

Global and regional brain age prediction:

Brain age prediction was used to estimate global and regional brain age based on the MRI data. In line with recent brain-age studies (***de Lange et al., 2020a***, ***2019***; ***Kaufmann et al., 2019***), the *XGBoost regressor model*, which is based on a decision-tree ensemble algorithm, was used to run the brain age prediction (https://xgboost.readthedocs.io/en/latest/python). XGboost includes advanced regularization to reduce overfitting (***Chen and Guestrin, 2016***), and uses a gradient boosting framework where the final model is based on a collection of individual models (https://github.com/dmlc/xgboost). Randomized search with ten folds and ten iterations was run to optimize parameters, using all imaging features as input. Scanned parameters ranges were set to *maximum depth*: [2, 10, 1], *number of estimators*: [60, 220, 40], and *learning rate*: [0.1, 0.01, 0.05]. The optimized parameters *maximum depth* = 6, *number of estimators* = 140, and *learning rate* = 0.1 were used for all subsequent models.

To replicate our findings described in ***de Lange et al.*** (***2019***), we trained a global brain-age prediction model using the part of the current sample that overlapped with the previous study (N = 10,907), and applied it to the newly added participants (N = 8880), before testing the association between number of previous childbirths and global brain age in the group of new participants. Note that the training set of 10,907 participants overlapping with the previous study showed a lower N relative to the sample in ***de Lange et al.*** (***2019***) due to correction for the variables listed in *sample characteristics*.

The full sample (19,787) was utilized to investigate regional brain aging. Averages of the right and left hemisphere measures were first calculated for each feature, and hierarcical clustering was performed on the Spearman rank-order correlation using Scikit-learn version 0.22.2 (https://scikit-learn.org/stable/modules/clustering.html#clustering). All features were grouped according to their associated cluster ID, and separate prediction models were run with ten-fold cross validation, providing cluster-specific brain age gap estimations (predicted age – chronological age) for each individual. To investigate model prediction accuracy, R^2, RMSE, and MAE were calculated for each model, and correlation analyses were run for predicted versus chronological age. The same procedure was followed for subclusters and region-specific brain age predictions.

Associations between previous childbirths and regional brain aging:

To investigate associations between number of previous childbirths and brain aging, separate regression analyses were run using cluster-specific brain age gap estimates as the dependent variable, and *number of childbirths* as independent variable. Chronological age was included as a co-

bioRxiv preprint doi: https://doi.org/10.1101/2020.05.08.084616; this version posted May 10, 2020. The copyright holder for this preprint (which was not certified by peer review) is the author/funder, who has granted bioRxiv a license to display the preprint in perpetuity. It is made available under a CC-BY-ND 4.0 International license.
Manuscript submitted to eLife

variate, adjusting for age-bias in the brain age predictions as well as age-dependence in number of childbirths (***Le et al., 2018***; ***de Lange and Cole, 2020***). *P*-values were corrected for multiple comparisons using false discovery rate (FDR) correction (***Benjamini and Hochberg, 1995***). To directly compare the associations, Z tests for correlated samples (***Zimmerman, 2012***) were run using

$$Z = (\beta_{m1} - \beta_{m2}) / \sqrt{\sigma_{m1}^2 + \sigma_{m2}^2 - 2\rho\sigma_{m1}\sigma_{m2}} \quad (1)$$

where "m1" and "m2" represent model 1 and 2, the β terms represent the beta value from the regression fits, the σ terms represent their errors, and ρ represents the correlation between the two sets of associations. The statistical analyses were conducted using Python 3.7.0.

Acknowledgements

This research was conducted using the UK Biobank under Application 27412. While working on this study, the authors received funding from the Research Council of Norway (AM.G.dL.; 286838, T.K.; 276082, L.T.W.; 273345, 249795, 298646, 300768, 223273), the South-East Norway Regional Health Authority (L.T.W.; 2015073, 2019107), the European Research Council under the European Union's Horizon 2020 research and innovation programme (L.T.W.; 802998), the Alzheimer's Society (S.S.; Grant Number 441), UK Medical Research Council (K.P.E.; G1001354), and the HDH Wills 1965 Charitable Trust (K.P.E: 1117747).

References

Alfaro-Almagro F, Jenkinson M, Bangerter NK, Andersson JL, Griffanti L, Douaud G, Sotiropoulos SN, Jbabdi S, Hernandez-Fernandez M, Vallee E, et al. Image processing and quality control for the first 10,000 brain imaging datasets from UK Biobank. Neuroimage. 2018; 166:400–424.

Barha CK, Galea LA. Influence of different estrogens on neuroplasticity and cognition in the hippocampus. Biochimica et Biophysica Acta (BBA)-General Subjects. 2010; 1800(10):1056–1067.

Barha CK, Galea LA. Motherhood alters the cellular response to estrogens in the hippocampus later in life. Neurobiology of aging. 2011; 32(11):2091–2095.

Barha CK, Galea LA. The maternal'baby brain'revisited. Nature neuroscience. 2017; 20(2):134.

Barha CK, Hanna CW, Salvante KG, Wilson SL, Robinson WP, Altman RM, Nepomnaschy PA. Number of children and telomere length in women: a prospective, longitudinal evaluation. PloS one. 2016; 11(1).

Barth C, de Lange AMG. Towards an understanding of women's brain aging: the immunology of pregnancy and menopause. . 2020; .

Beeri MS, Rapp M, Schmeidler J, Reichenberg A, Purohit DP, Perl DP, Grossman HT, Prohovnik I, Haroutunian V, Silverman JM. Number of children is associated with neuropathology of Alzheimer's disease in women. Neurobiology of aging. 2009; 30(8):1184–1191.

Benjamini Y, Hochberg Y. Controlling the false discovery rate: a practical and powerful approach to multiple testing. Journal of the Royal statistical society: series B (Methodological). 1995; 57(1):289–300.

Boddy AM, Fortunato A, Wilson Sayres M, Aktipis A. Fetal microchimerism and maternal health: a review and evolutionary analysis of cooperation and conflict beyond the womb. BioEssays. 2015; 37(10):1106–1118.

Breiman L. Random forests. Machine learning. 2001; 45(1):5–32.

Brunton PJ, Russell JA. The expectant brain: adapting for motherhood. Nature Reviews Neuroscience. 2008; 9(1):11–25.

Champagne FA, Chretien P, Stevenson CW, Zhang TY, Gratton A, Meaney MJ. Variations in nucleus accumbens dopamine associated with individual differences in maternal behavior in the rat. Journal of Neuroscience. 2004; 24(17):4113–4123.

Chan WF, Gurnot C, Montine TJ, Sonnen JA, Guthrie KA, Nelson JL. Male microchimerism in the human female brain. PLoS One. 2012; 7(9):e45592.

Chen T, Guestrin C. Xgboost: A scalable tree boosting system. In: *Proceedings of the 22nd acm sigkdd international conference on knowledge discovery and data mining*; 2016. p. 785–794.

bioRxiv preprint doi: https://doi.org/10.1101/2020.05.08.084616; this version posted May 10, 2020. The copyright holder for this preprint (which was not certified by peer review) is the author/funder, who has granted bioRxiv a license to display the preprint in perpetuity. It is made available under a CC-BY-NC-ND 4.0 International license.

334 **Cole JH**. Multi-modality neuroimaging brain-age in UK Biobank: relationship to biomedical, lifestyle and cogni-
335 tive factors. bioRxiv. 2019; https://www.biorxiv.org/content/early/2019/10/21/812982, doi: 10.1101/812982.

336 **Cole JH**, Franke K. Predicting age using neuroimaging: innovative brain ageing biomarkers. Trends in neuro-
337 sciences. 2017; 40(12):681–690.

338 **Cole JH**, Marioni RE, Harris SE, Deary IJ. Brain age and other bodily 'ages': implications for neuropsychiatry.
339 Molecular psychiatry. 2019; 24(2):266–281.

340 **Cole JH**, Poudel RP, Tsagkrasoulis D, Caan MW, Steves C, Spector TD, Montana G. Predicting brain age with deep
341 learning from raw imaging data results in a reliable and heritable biomarker. NeuroImage. 2017; 163:115–
342 124.

343 **Cole JH**, Ritchie SJ, Bastin ME, Hernández MV, Maniega SM, Royle N, Corley J, Pattie A, Harris SE, Zhang Q, et al.
344 Brain age predicts mortality. Molecular psychiatry. 2018; 23(5):1385.

345 **Colucci M**, Cammarata S, Assini A, Croce R, Clerici F, Novello C, Mazzella L, Dagnino N, Mariani C, Tanganelli P.
346 The number of pregnancies is a risk factor for Alzheimer's disease. European Journal of Neurology. 2006;
347 13(12):1374–1377.

348 **Desikan RS**, Ségonne F, Fischl B, Quinn BT, Dickerson BC, Blacker D, Buckner RL, Dale AM, Maguire RP, Hyman
349 BT, et al. An automated labeling system for subdividing the human cerebral cortex on MRI scans into gyral
350 based regions of interest. Neuroimage. 2006; 31(3):968–980.

351 **Duarte-Guterman P**, Leuner B, Galea LA. The long and short term effects of motherhood on the brain. Fron-
352 tiers in neuroendocrinology. 2019; .

353 **Eavani H**, Habes M, Satterthwaite TD, An Y, Hsieh MK, Honnorat N, Erus G, Doshi J, Ferrucci L, Beason-Held
354 LL, et al. Heterogeneity of structural and functional imaging patterns of advanced brain aging revealed via
355 machine learning methods. Neurobiology of aging. 2018; 71:41–50.

356 **Eid RS**, Chaiton JA, Lieblich SE, Bodnar TS, Weinberg J, Galea LA. Early and late effects of maternal experience
357 on hippocampal neurogenesis, microglia, and the circulating cytokine milieu. Neurobiology of aging. 2019;
358 78:1–17.

359 **Ferris CF**, Kulkarni P, Sullivan JM, Harder JA, Messenger TL, Febo M. Pup suckling is more rewarding than co-
360 caine: evidence from functional magnetic resonance imaging and three-dimensional computational analysis.
361 Journal of Neuroscience. 2005; 25(1):149–156.

362 **Fischl B**, Salat DH, Busa E, Albert M, Dieterich M, Haselgrove C, Van Der Kouwe A, Killiany R, Kennedy D, Klave-
363 ness S, et al. Whole brain segmentation: automated labeling of neuroanatomical structures in the human
364 brain. Neuron. 2002; 33(3):341–355.

365 **Fleming AS**, Cheung U, Myhal N, Kessler Z. Effects of maternal hormones on 'timidity'and attraction to pup-
366 related odors in female rats. Physiology & behavior. 1989; 46(3):449–453.

367 **Fox M**, Berzuini C, Knapp LA, Glynn LM. Women's Pregnancy Life History and Alzheimer's Risk: Can Immunoreg-
368 ulation Explain the Link? American Journal of Alzheimer's Disease & Other Dementias®. 2018; 33(8):516–526.

369 **Franke K**, Gaser C. Ten Years of BrainAGE as a Neuroimaging Biomarker of Brain Aging: What Insights Have
370 We Gained? Frontiers in Neurology. 2019; 10:789.

371 **Galea LA**, Leuner B, Slattery DA. Hippocampal plasticity during the peripartum period: influence of sex steroids,
372 stress and ageing. Journal of neuroendocrinology. 2014; 26(10):641–648.

373 **Haber SN**, Knutson B. The reward circuit: linking primate anatomy and human imaging. Neuropsychopharma-
374 cology. 2010; 35(1):4–26.

375 **Hillerer KM**, Jacobs VR, Fischer T, Aigner L. The maternal brain: an organ with peripartal plasticity. Neural
376 plasticity. 2014; 2014.

377 **Hoekzema E**, Barba-Müller E, Pozzobon C, Picado M, Lucco F, García-García D, Soliva JC, Tobeña A, Desco M,
378 Crone EA, et al. Pregnancy leads to long-lasting changes in human brain structure. Nature Neuroscience.
379 2017; 20(2):287.

380 **Hoekzema E**, Tamnes CK, Berns P, Barba-Müller E, Pozzobon C, Picado M, Lucco F, Martínez-García M, Desco
381 M, Ballesteros A, et al. Becoming a mother entails anatomical changes in the ventral striatum of the human
382 brain that facilitate its responsiveness to offspring cues. Psychoneuroendocrinology. 2020; 112:104507.

bioRxiv preprint doi: https://doi.org/10.1101/2020.05.08.084616; this version posted May 10, 2020. The copyright holder for this preprint (which was not certified by peer review) is the author/funder, who has granted bioRxiv a license to display the preprint in perpetuity. It is made available under a CC-BY-ND 4.0 International license.

Jang H, Bae JB, Dardiotis E, Scarmeas N, Sachdev PS, Lipnicki DM, Han JW, Kim TH, Kwak KP, Kim BJ, et al. Differential effects of completed and incomplete pregnancies on the risk of Alzheimer disease. Neurology. 2018; 91(7):e643–e651.

Kaufmann T, van der Meer D, Doan NT, Schwarz E, Lund MJ, Agartz I, Alnæs D, Barch DM, Baur-Streubel R, Bertolino A, et al. Common brain disorders are associated with heritable patterns of apparent aging of the brain. Nature Neuroscience, In press. 2019; .

Kieffer TE, Faas MM, Scherjon SA, Prins JR. Pregnancy persistently affects memory T cell populations. Journal of reproductive immunology. 2017; 119:1–8.

Kim P, Dufford AJ, Tribble RC. Cortical thickness variation of the maternal brain in the first 6 months postpartum: associations with parental self-efficacy. Brain Structure and Function. 2018; 223(7):3267–3277.

Kim P, Leckman JF, Mayes LC, Feldman R, Wang X, Swain JE. The plasticity of human maternal brain: longitudinal changes in brain anatomy during the early postpartum period. Behavioral neuroscience. 2010; 124(5):695.

Kinsley CH, Lambert KG. Reproduction-induced neuroplasticity: Natural behavioural and neuronal alterations associated with the production and care of offspring. Journal of neuroendocrinology. 2008; 20(4):515–525.

Kinsley CH, Trainer R, Stafisso-Sandoz G, Quadros P, Marcus LK, Hearon C, Meyer EAA, Hester N, Morgan M, Kozub FJ, et al. Motherhood and the hormones of pregnancy modify concentrations of hippocampal neuronal dendritic spines. Hormones and behavior. 2006; 49(2):131–142.

Kinsley CH, Bardi M, Karelina K, Rima B, Christon L, Friedenberg J, Griffin G. Motherhood induces and maintains behavioral and neural plasticity across the lifespan in the rat. Archives of sexual behavior. 2008; 37(1):43.

de Lange AMG, Anatürk M, Kaufmann T, Cole JH, Griffanti L, Zsoldos E, Jensen D, Suri S, Filippini N, Singh-Manoux A, et al. Multimodal brain-age prediction and cardiovascular risk: The Whitehall II MRI sub-study. bioRxiv. 2020; .

de Lange AMG, Barth C, Kaufmann T, Maximov II, van der Meer D, Agartz I, Westlye LT. Women's brain aging: effects of sex-hormone exposure, pregnancies, and genetic risk for Alzheimer's disease. bioRxiv. 2020; p. 826123.

de Lange AMG, Cole JH. Commentary: Correction procedures in brain-age prediction. NeuroImage: Clinical. 2020; 26.

de Lange AMG, Kaufmann T, van der Meer D, Maglanoc LA, Alnæs D, Moberget T, Douaud G, Andreassen OA, Westlye LT. Population-based neuroimaging reveals traces of childbirth in the maternal brain. Proceedings of the National Academy of Sciences. 2019; .

Le TT, Kuplicki RT, McKinney BA, Yeh Hw, Thompson WK, Paulus MP, Investigators T, et al. A nonlinear simulation framework supports adjusting for age when analyzing BrainAGE. Frontiers in aging neuroscience. 2018; 10.

Lisofsky N, Wiener J, de Condappa O, Gallinat J, Lindenberger U, Kühn S. Differences in navigation performance and postpartal striatal volume associated with pregnancy in humans. Neurobiology of learning and memory. 2016; 134:400–407.

Love G, Torrey N, McNamara I, Morgan M, Banks M, Hester NW, Glasper ER, DeVries AC, Kinsley CH, Lambert KG. Maternal experience produces long-lasting behavioral modifications in the rat. Behavioral neuroscience. 2005; 119(4):1084.

Luders E, Kurth F, Gingnell M, Engman J, Yong EL, Poromaa IS, Gaser C. From Baby Brain to Mommy Brain: Widespread Gray Matter Gain After Giving Birth. Cortex. 2020; .

Miller KL, Alfaro-Almagro F, Bangerter NK, Thomas DL, Yacoub E, Xu J, Bartsch AJ, Jbabdi S, Sotiropoulos SN, Andersson JL, et al. Multimodal population brain imaging in the UK Biobank prospective epidemiological study. Nature neuroscience. 2016; 19(11):1523.

Mishra A, Brinton RD. Inflammation: bridging age, menopause and APOEε4 genotype to alzheimer's disease. Frontiers in aging neuroscience. 2018; 10.

Mowinckel AM, Vidal-Piñeiro D. Visualisation of Brain Statistics with R-packages ggseg and ggseg3d. arXiv preprint arXiv:191208200. 2019; .

bioRxiv preprint doi: https://doi.org/10.1101/2020.05.08.084616; this version posted May 10, 2020. The copyright holder for this preprint (which was not certified by peer review) is the author/funder, who has granted bioRxiv a license to display the preprint in perpetuity. It is made available under a CC-BY-NC-ND 4.0 International license.

Natri H, Garcia AR, Buetow KH, Trumble BC, Wilson MA. The Pregnancy Pickle: Evolved Immune Compensation Due to Pregnancy Underlies Sex Differences in Human Diseases. Trends in Genetics. 2019; 35(7):478–488.

Nott P, Franklin M, Armitage C, Gelder M. Hormonal changes and mood in the puerperium. The British Journal of Psychiatry. 1976; 128(4):379–383.

Numan M, Woodside B. Maternity: neural mechanisms, motivational processes, and physiological adaptations. Behavioral neuroscience. 2010; 124(6):715.

Oatridge A, Holdcroft A, Saeed N, Hajnal JV, Puri BK, Fusi L, Bydder GM. Change in brain size during and after pregnancy: study in healthy women and women with preeclampsia. American Journal of Neuroradiology. 2002; 23(1):19–26.

Paul S, Austin J, Elliott R, Ellison-Wright I, Wan MW, Drake R, Downey D, Elmadih A, Mukherjee I, Heaney L, et al. Neural pathways of maternal responding: systematic review and meta-analysis. Archives of women's mental health. 2019; 22(2):179–187.

Robinson DL, Zitzman DL, Williams SK. Mesolimbic dopamine transients in motivated behaviors: focus on maternal behavior. Frontiers in psychiatry. 2011; 2:23.

Rocchetti M, Radua J, Paloyelis Y, Xenaki LA, Frascarelli M, Caverzasi E, Politi P, Fusar-Poli P. Neurofunctional maps of the 'maternal brain'and the effects of oxytocin: A multimodal voxel-based meta-analysis. Psychiatry and clinical neurosciences. 2014; 68(10):733–751.

Rolls A, Schori H, London A, Schwartz M. Decrease in hippocampal neurogenesis during pregnancy: a link to immunity. Molecular psychiatry. 2008; 13(5):468.

Rosen AF, Roalf DR, Ruparel K, Blake J, Seelaus K, Villa LP, Ciric R, Cook PA, Davatzikos C, Elliott MA, et al. Quantitative assessment of structural image quality. Neuroimage. 2018; 169:407–418.

Schock H, Zeleniuch-Jacquotte A, Lundin E, Grankvist K, Lakso HÅ, Idahl A, Lehtinen M, Surcel HM, Fortner RT. Hormone concentrations throughout uncomplicated pregnancies: a longitudinal study. BMC pregnancy and childbirth. 2016; 16(1):146.

Simerly RB. Wired for reproduction: organization and development of sexually dimorphic circuits in the mammalian forebrain. Annual review of neuroscience. 2002; 25(1):507–536.

Smith SM, Elliott LT, Alfaro-Almagro F, McCarthy P, Nichols TE, Douaud G, Miller KL. Brain aging comprises multiple modes of structural and functional change with distinct genetic and biophysical associations. eLife. 2020; 9:e52677.

Smith SM, Vidaurre D, Alfaro-Almagro F, Nichols TE, Miller KL. Estimation of brain age delta from brain imaging. NeuroImage. 2019; .

Voevodskaya O, Simmons A, Nordenskjöld R, Kullberg J, Ahlström H, Lind L, Wahlund LO, Larsson EM, Westman E, Initiative ADN, et al. The effects of intracranial volume adjustment approaches on multiple regional MRI volumes in healthy aging and Alzheimer's disease. Frontiers in aging neuroscience. 2014; 6:264.

Whitacre CC, Reingold SC, O'Looney PA, Blankenhorn E, Brinley F, Collier E, Duquette P, Fox H, Giesser B, Gilmore W, et al. A gender gap in autoimmunity: task force on gender, multiple sclerosis and autoimmunity. Science. 1999; 283(5406):1277–1278.

Wilks SS. The large-sample distribution of the likelihood ratio for testing composite hypotheses. The annals of mathematical statistics. 1938; 9(1):60–62.

Xerri C, Stern JM, Merzenich MM. Alterations of the cortical representation of the rat ventrum induced by nursing behavior. Journal of Neuroscience. 1994; 14(3):1710–1721.

Zeng XX, Tan KH, Yeo A, Sasajala P, Tan X, Xiao ZC, Dawe G, Udolph G. Pregnancy-associated progenitor cells differentiate and mature into neurons in the maternal brain. Stem cells and development. 2010; 19(12):1819–1830.

Zeng Y, Ni Zm, Liu Sy, Gu X, Huang Q, Liu Ja, Wang Q. Parity and all-cause mortality in women and men: a dose-response meta-analysis of cohort studies. Scientific reports. 2016; 6:19351.

Zimmerman DW. Correcting Two-Sample" z" and" t" Tests for Correlation: An Alternative to One-Sample Tests on Difference Scores. Psicologica: International Journal of Methodology and Experimental Psychology. 2012; 33(2):391–418.